FULL PAPER

BJC

British Journal of Cancer (2014) 110, 636–647 | doi: 10.1038/bjc.2013.764

Keywords: medulloblastoma; miRNA-9; epigenetic silencing; paediatric cancer

# Epigenetic silencing of miRNA-9 is associated with HES1 oncogenic activity and poor prognosis of medulloblastoma

G Fiaschetti[1,9], L Abela[2,9], N Nonoguchi[3,9], A M Dubuc[4], M Remke[5], A Boro[6], E Grunder[2], U Siler[7], H Ohgaki[3], M D Taylor[8], M Baumgartner[1], T Shalaby[1] and M A Grotzer*[,2]

[1]*Neuro-Oncology group, Experimental Infectious Diseases and Cancer Research, August-Forel Strasse 1, Zurich CH-8008, Switzerland;* [2]*Division of Oncology, University Children's Hospital of Zürich, Steinwiesstrasse 75, Zurich CH-8032, Switzerland;* [3]*International Agency for Research on Cancer, World Health Organization, Section of Molecular Pathology, 150 Cours Albert Thomas, 69372, Lyon Cedex 08, France;* [4]*Arthur and Sonia Labatt Brain Tumour Research Centre, MaRS Centre – 11-401M, 101 College Street, Toronto, ON M5G1L7, Canada;* [5]*Brain Tumor Research Centre, 101 College Street, TMDT-11-401M, Toronto, ON M5G1L7, Canada;* [6]*Oncology group, Experimental Infectious Diseases and Cancer Research, August-Forel Strasse 1, Zurich CH-8008, Switzerland;* [7]*Division of Immunology, University Children's Hospital of Zürich, Steinwiesstrasse 75, Zurich CH-8032, Switzerland and* [8]*The Hospital for Sick Children, Division of Neurosurgery, Suite 1504, 555 University Avenue, Toronto, ON M5G1X8, Canada*

**Background:** microRNA-9 is a key regulator of neuronal development aberrantly expressed in brain malignancies, including medulloblastoma. The mechanisms by which microRNA-9 contributes to medulloblastoma pathogenesis remain unclear, and factors that regulate this process have not been delineated.

**Methods:** Expression and methylation status of microRNA-9 in medulloblastoma cell lines and primary samples were analysed. The association of microRNA-9 expression with medulloblastoma patients' clinical outcome was assessed, and the impact of microRNA-9 restoration was functionally validated in medulloblastoma cells.

**Results:** microRNA-9 expression is repressed in a large subset of MB samples compared with normal fetal cerebellum. Low microRNA-9 expression correlates significantly with the diagnosis of unfavourable histopathological variants and with poor clinical outcome. microRNA-9 silencing occurs via cancer-specific CpG island hypermethylation. HES1 was identified as a direct target of microRNA-9 in medulloblastoma, and restoration of microRNA-9 was shown to trigger cell cycle arrest, to inhibit clonal growth and to promote medulloblastoma cell differentiation.

**Conclusions:** microRNA-9 is a methylation-silenced tumour suppressor that could be a potential candidate predictive marker for poor prognosis of medulloblastoma. Loss of microRNA-9 may confer a proliferative advantage to tumour cells, and it could possibly contribute to disease pathogenesis. Thus, re-expression of microRNA-9 may constitute a novel epigenetic regulation strategy against medulloblastoma.

Medulloblastoma (MB) is the most common malignant brain tumour in children. Despite recent treatment advances, approximately 30% of children with MB will die from their disease (Northcott *et al*, 2012a). Those who survive often have a significantly reduced quality of life as result of therapy-related sequelae (Mulhern *et al*, 2005). Novel and targeted therapeutic

*Correspondence: Professor Dr MA Grotzer; E-mail: Michael.Grotzer@kispi.uzh.ch
[9]These authors contributed equally to this work.

Revised 31 October 2013; accepted 13 November 2013; published online 17 December 2013

strategies are thus needed to reduce mortality and morbidity. Recently, molecular profiling studies identified four core subgroups of MB tumours with potential targets for specific therapies based on varying gene expression (Kool *et al*, 2008; Northcott *et al*, 2011). WNT tumours are characterised by activated wingless pathway and carry a favourable prognosis under current treatment regimens. SHH tumours possess active hedgehog signalling and have an intermediate prognosis. Group 3, characterised by high MYC levels, and Group 4 tumours, molecularly less well characterised, are usually associated with poor prognosis (Taylor *et al*, 2012). Despite the great advance in the fight against MB resulting from molecular-based sub-grouping, additional efforts are needed to identify key biological alterations that could be targeted by tailored therapies.

MicroRNAs (miRNAs) are small RNA molecules that have emerged as key regulators during the development of both normal human brain and brain tumours, including MB (Hummel *et al*, 2011; Dubuc *et al*, 2012). Upon binding to the 3′ UTR, miRNAs downregulate the target genes expression by blocking the translation and/or by inducing mRNA degradation. Recently, specific miRNA expression signatures helped improving the molecular classification of brain tumours and facilitated the diagnosis and prediction of therapy response and prognosis (Fernandez *et al*, 2009). miRNAs are suggested to have a critical role in MB tumour pathogenesis because of their altered expression observed in a large number of MB primary samples (Pang *et al*, 2009; Turner *et al*, 2010). A high throughput expression profile of miRNAs expressed either in neuronal tissues or associated with tumour development revealed a tumour-specific pattern of microRNAs expression in human primary MB samples (Ferretti *et al*, 2009). In particular, miR-9 was found to be one of the key miRNAs expressed at low levels in MB tumours compared with normal fetal cerebellum.

MiR-9 is a regulator of neuronal progenitor cell fate during neurogenesis (Wienholds *et al*, 2005; Shibata *et al*, 2011), which has recently been implicated in cancer (Delaloy *et al*, 2010). Although most studies indicate a tumour-suppressor activity for *miR-9* in cancer cells (Laios *et al*, 2008), conflicting data exist, and the outcome of *miR-9* function appears to be tumour specific (Khew-Goodall and Goodall, 2010). *miR-9* is downregulated in breast cancer, renal cell carcinoma, and gastric cancer due to promoter methylation (Lehmann *et al*, 2008; Hildebrandt *et al*, 2010; Tsai *et al*, 2011). In contrast, *miR-9* has been found to be upregulated in gliomas and in colorectal cancer (Malzkorn *et al*, 2010; Zhu *et al*, 2012). Recent studies also report that *miR-9* is heterogeneously expressed within a given tissue (Bonev *et al*, 2011). To date, it remains unclear how aberrant *miR-9* expression contributes to MB pathogenesis. Therefore, we investigated the expression of *miR-9* in MB, its functional role, and its association with the clinical outcome of MB patients.

## MATERIALS AND METHODS

**Human MB primary samples and cell lines.** The tumour material used in this study originates from two sets of archival MB samples from patients treated at the University Children's Hospital of Zürich, Zürich, Switzerland ($n = 78$; 63 formalin-fixed paraffin-embedded + 15 fresh frozen). DNA from 64 MB samples (49 formalin-fixed paraffin-embedded + 15 fresh frozen) was available for the methylation study. mRNA was available from 14 out of the 63 formalin-fixed paraffin-embedded samples and from 15 additional fresh frozen MB samples. All tissue specimens used in the study were obtained from the Swiss Pediatric Oncology Group (SPOG) Tumour Bank. Written informed consent was obtained from each patient by the hospital that provided the tissue samples. The use of SPOG Tumour Bank tissue samples for cancer research purposes was approved by the Ethical Review Board of Zurich (Ref. No. StV-18/02). Gene expression profile of 88 primary MB tumour samples was performed in Dr. Taylor's Lab (The Hospital for Sick Children, Division of Neurosurgery, Toronto, ON, Canada) and used for gene expression and survival analysis. Normal fetal cerebella were used as control for the mRNA expression studies ($n = 5$; gestational age: 16–26 weeks). Publicly available microarray data from 285 primary MB samples was used to determine the correlation between the expression of selected genes (Northcott *et al*, 2012b). MB expression profiles were generated on Affymetrix Human Gene 1.1 ST Array (Santa Clara, CA, USA). Data are accessible through the open access database R2 for visualisation and analysis of microarray data (http://r2.amc.nl).

MB cell lines were cultured as previously published (von Bueren *et al*, 2007) and maintained at 37 °C in a humidified atmosphere with 5% $CO_2$. DAOY human MB cells were purchased from American Type Culture Collection (Manassas, VA, USA). D341, D425, UW-228-2 and Med-1 human MB cells were the kind gift of Dr Henry Friedman (Duke University, Durham, UK). PFSK cells were the kind gift of Dr Peter Phillips (Children's Hospital of Philadelphia, Philadelphia, PA, USA).

**MicroRNA and RNA analysis and expression profiling of human primary MBs.** Total RNA for microRNA analysis was isolated using the mirVana miRNA Isolation Kit (Ambion, Life Technology, NY, USA) according to the manufacturer's instructions. First-strand synthesis of mature microRNAs was followed by qRT–PCR using microRNA-specific TaqMan MGB probes for *miR-9* (ID 000583) and, for control RNA, U6 small nuclear 2 (RNU6B) (ID 001093) (Applied Biosystems, Life Technology, Carlsbad, CA, USA). Total RNA for mRNA analysis was extracted using the RNeasy Mini Kit (Qiagen, Basel, Switzerland) following the manufacturer's instructions. For the qRT–PCR reaction, the Gene Expression Master Mix was used, and the protocol was optimised for the ABI7900HT reader (Applied Biosystems, Life Technology). Probe-primer solutions specific for the following genes were used: *HES1* (Hs00172878_m1), *p21* (Hs00355782_m1), *MASH1/ASCL1* (Hs00269932_m1), *NEUROD1* (Hs00159598_m1), *MAP2* (Hs00258900_m1), *NEFH* (Hs00606024_m1), *GFAP* (Hs00909236_m1), *NES* (Hs00707120_s1), and *TUBB3* (Hs00964962_g1). Normal human cerebellum was used as a reference (Clontech-Takara Bio Europe, Saint-Germain-en-Laye, France). The relative gene expression was calculated for each gene of interest by using the $\Delta\Delta C_T$ method, where cycle threshold ($C_T$) values were normalised to the housekeeping genes RNA, U6 small nuclear 2 (*RNU6B*), succinate dehydrogenase complex subunit A (*SDHA*) (Hs00188166_m1), and 18S (Hs99999901_s1) (Applied Biosystems, Life Technology).

**Promoter methylation analysis of the *miR-9*genes.** Promoter methylation status of the *miR-9-1*, *-2*, and *-3* genes was analysed by methylation-specific PCR (MSP) in MB cell lines and 64 primary samples of MB tissues. Bisulfite conversion of DNA was carried out using the EZ DNA Methylation Kit (Zymo Research Co., Irvine, CA, USA) following the manufacturer's instructions. The primers and the protocol used for MS-PCR have been previously described (Lujambio *et al*, 2008; Bandres *et al*, 2009). For each MS-PCR reaction, universal methylated DNA (Chemicon International, Temecula, CA, USA) was included as positive control and normal lymphocyte DNA as negative control. Samples of normal tissue on paraffin sections were used as negative controls. PCR products were run on a 3% agarose gel and were visualised with UV trans-illumination (Bio-Rad, Hercules, CA, USA). Methylated bands were detectable if >25% of the DNA was methylated. Similarly, methylated bands were not detectable when all DNA was unmethylated and, vice versa, confirming the sensitivity and specificity of the method.

**In silico search for *miR-9* target genes.** Predictions on miR-9-HES1 interactions were extracted either from databases that predict miRNA target sequences, for example, TargetScan (Lewis *et al*, 2003), Pictar (Krek *et al*, 2005), DIANA-microT 3.0 algorithm (Maragkakis *et al*, 2009) and microRNA.org (Betel *et al*, 2008) or from databases that can predict miRNA binding sites on potential target genes, such as StarBase v2.0 (Yang *et al*, 2011), microPIR (Piriyapongsa *et al*, 2012), and miRWalk (Dweep *et al*, 2011).

**Western blotting and immunofluorescence analysis.** Western blotting analyses were performed as previously published (Fiaschetti *et al*, 2011). The membranes were incubated with the following first antibodies: HES1 (H-140) (sc-25392, Santa Cruz Biotechnology, Santa Cruz, CA, USA), $\beta$-tubulin Class III (TUBB3) (2G10) (Ab78078, Abcam, Cambridge, UK), MASH1/Achaete-scute homolog 1 (ab38557, Abcam), and Cip1/WAF-1/p21 (CP74) (P1484, Sigma-Aldrich, Buchs, Switzerland). Protein detection was performed with Supersignal Western Bio Chemo-luminescent Substrate (Pierce, Thermo Fisher Scientific, Rockford, IL, USA). $\beta$-Actin (AC-74) (A5316, Sigma-Aldrich) was used as a loading control. For immunofluorescence staining, cells were fixed in 4% PFA and blocked in medium containing 10% FCS and 0.5% Triton. Cells were stained over night at 4 °C for NES (196908) (MAB1259, R&D Systems, Minneapolis, MN, USA) and TUBB3 (Ab78078, Abcam). Alexa Fluor 488 or 594 (1/200) (Invitrogen, Life Technology) antibodies were used as secondary antibodies. All stainings were analysed with an Axioskop2 mot plus fluorescence microscope (Zeiss, Jena, Germany).

**Cell cycle and apoptosis analysis.** MB cells were harvested, PBS washed, and immediately fixed in 5 ml ice-cold 70% ethanol. Before flow cytometry analysis, cells were resuspended in 300 $\mu$l propidium iodide solution, 2 $\mu$l of RNase (100 mg ml$^{-1}$) was added, and the cells were incubated at 37 °C for 45 min. Flow cytometry analysis was performed on a BD FACS Canto II instrument (BD Biosciences, Franklin Lakes, NJ, USA) following the manufacturer's recommended protocol. Data were collected with DIVA software (BD Biosciences) and analysed with FlowJo software (TreeStar Inc., Ashland, OR, USA) using appropriate controls and gates.

Activation of caspases 3 and 7 was detected using the Caspase-Glo 3/7 Assay (Promega Corporation, Madison, WI, USA). Annexin V–APC staining (550475, BD Biosciences) was measured by flow cytometry. Apoptosis induction was confirmed by quantifying hystone-associated DNA fragments by Cell Death Detection ELISA$^{PLUS}$ assay (Roche Diagnostics, Rotkreuz, Switzerland).

**Cell transfection and 5-Aza-2′-deoxycytidine (5-Aza) treatment.** Cells were seeded in six-well plates at a cell density of $4 \times 10^4$ (DAOY, PFSK) and $2 \times 10^5$ (D341, D425), respectively. Transfection of pre-*miR-9* (PM10022, Ambion) or negative control oligonucleotide referred to as scrambled (AM17110, Ambion) in a final concentration of 30 nmol l$^{-1}$ was performed using siPORT NeoFX transfection reagent (Ambion) according to the manufacturer's recommendations. Transfection efficiency was assessed with a FAM-labeled pre-*miR-9* negative control (AM17121, Ambion) 24 h post transfection. FAM-positive cells were counted under a fluorescence microscope and expressed as a percentage of total cells. Six random fields were counted for each sample. DAOY and PFSK cells (70–80% confluent) were transfected using *HES1* siRNA (ID 6922, Ambion, Silencer select pre-designed siRNA) at 20 nM final concentration. As control, Silencer Negative Control siRNA no. 1 (AM4611, Ambion) was used under the same conditions. Cells were harvested 48 and 72 h after transfection for subsequent quantitative qRT–PCR and western blotting analysis. Cells were plated in six-well plates and treated with 0.1 mM 5-Aza (A3656; Sigma-Aldrich) or control (DMSO) for 24–48 h before further analysis.

**Construction of 3′UTR reporter plasmids and luciferase assays.** A 459-bp fragment of the 3′UTR of *HES1* containing the putative *miR-9* binding site wasPCR-amplified from PFSK cell's genomic DNA (FW: 5′-AAAACTCGAGAACGCAGTGTCACCTTCC-3′, RE: 5′-AAAACTCGAGCAGTTCGAAGACATAAAAGCC-3′). The 459-base pair segment was designed to contain XhoI and NotI sites and was cloned into the psiCHECK-2 vector (Promega Corporation), between the XhoI and NotI site, immediately 3′ downstream of the renilla luciferase gene. All constructs were verified by DNA sequencing. Ten nanograms of psiCHECK-2 construct was co-transfected with 10 nM *miR-9* duplex or scrambled duplex into HEK-293T cells in a 96-well plate using lipofectamin-2000 (Invitrogen). After 48 h, the cell extract was obtained; firefly and renilla luciferase activities were measured with the Dual-Luciferase reporter system (Promega Corporation) according to the manufacturer's instructions.

**Statistical analysis.** All experiments were performed at least in triplicates. Data are represented as mean ± s.d. For *in vitro* experiments Student's t-test was used. *P*-values of $<0.05$ were considered significant. Pearson's correlation test was used for gene correlation in patient's samples.

## RESULTS

**Tumour-specific CpG island hypermethylation downregulates the expression of *miR-9* in MB cells.** To gain insight into the expression of *miR-9* in MB, we analysed a cohort of MB primary samples ($n=29$) and six MB-derived cell lines. Compared with normal human fetal cerebellum, a decreased expression level of *miR-9* was observed in the majority of MB tumour tissues (Figure 1A, and Supplementary Figure S1A) and in all the six MB cell lines tested (Figure 1B, upper panel). To confirm that *miR-9* downregulation is a common feature in MB, we validated our findings in an independent, non-overlapping cohort of primary MBs ($n=88$) with molecular subgroup information. *miR-9* expression was found to be lower in a large subset of MB tumour samples (91%, 80/88) than in normal fetal cerebellum, regardless of their genetic backgrounds (Figure 1C). Across the four MB molecular subtypes, *miR-9* downregulation was most pronounced in WNT and Group 3 subgroups, which are characterised by high expression of the *MYC* proto-oncogene (Figure 1C and Supplementary Figures S1B and C). In contrast, Group 4 tumours, which are characterised by the expression of high levels of genes involved in neuronal differentiation, displayed higher miR-9 levels than other subgroups that are comparable to normal cerebellar samples.

Tumour-suppressor genes can be inactivated in various ways, including CpG promoter hypermethylation (Esteller, 2002). Our preliminary investigation revealed no deletions in *miR-9* genes in MB cells (Supplementary Figure S1D). To determine whether hypermethylation caused reduced *miR-9* expression in MB cells, we examined methylation of the promoter regions of hsa-*miR-9* by MSP. Hsa-*miR-9* is represented by three genomic loci hsa-*miR-9-1* (1q22), hsa-*miR-9-2* (5q14.3), and hsa-*miR-9-3* (15q26.1) (Bandres *et al*, 2009). All three loci could independently contribute to the expression of *miR-9*. In contrast to the normal cerebellum, the three miR-9 loci were independently methylated in the subset of primary samples with low miR-9 expression and in all the tested MB cell lines (Figure 1A and B, lower panels).

To establish the causal relationship between methylation and the low *miR-9* expression level, we treated MB cells with the demethylating agent 5-Aza. After treatment with 5-Aza, *miR-9* expression markedly increased in all MB cell lines except in D341 cells, where only a small increase was observed (Figure 1D),

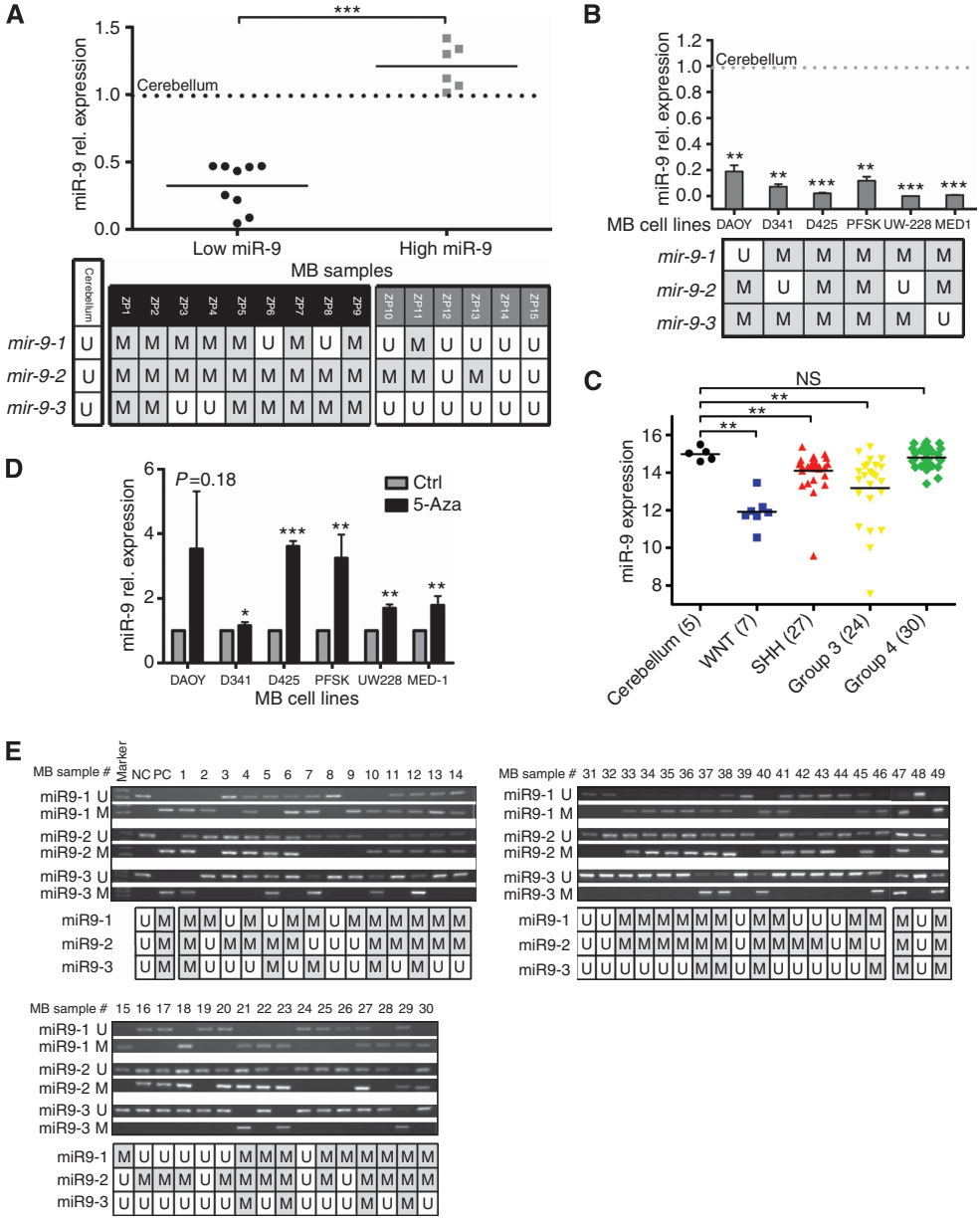


Figure 1. Expression of *miR-9* is epigenetically repressed in MB cells. Relative *miR-9* expression as determined by qRT–PCR (**A**) in 15 fresh, frozen MB primary samples and (**B**) in the indicated MB cell lines. Values represent the fold decrease of *miR-9-2* mRNA expression relative to normal cerebellum. Dotted line indicates cerebellum level at arbitrary value = 1. (**A** and **B**, lower panels) Methylation status of the three *miR-9* genes in the correspondent MB samples and cell lines. (**C**) Box plots showing relative expression of *miR-9-2* across MB subgroups compared with fetal cerebellum. Relative expression is a measure of the luminosity of the gene probe signal, corrected for the background luminosity of each array and normalised using control probes across different arrays. (**D**) qRT–PCR analysis of *miR-9* in the indicated human MB cell lines treated with 5-Aza or control (DMSO). (*$P<0.05$, **$P<0.01$, ***$P<0.001$ according to Student's *t*-test.) (**E**) Agarose gel showing MS-PCR products of the three *miR-9* genes' CpG island regions in 49 FFPE MB primary samples. Lower panel represents methylation status of the three *miR-9* genes in the correspondent MB samples. Abbreviations: M = methylated; NC = negative control; NS = not significant; PC = positive control; U = unmethylated.

confirming the role of promoter methylation in *miR-9* silencing. To determine the role of epigenetic regulation of hsa-*miR-9* in a clinically more relevant model, the promoter methylation status of the three has-*miR-9* genes was analysed in a panel of 64 MB samples using MSP analysis. In 78% (50/64) of MB patients, at least one of the three *miR-9* loci showed promoter methylation (Figure 1A, lower panel, and 1E). In particular, the promoter regions of *miR-9-1* were methylated in 64% (41/64) and *miR-9-2* was methylated in 73% (47/64), whereas *miR-9-3* promoter was methylated in 34% (23/64) of MB cases. These results indicate that the reduced expression of *miR-9* found in MB tissue samples and cell lines is likely caused by aberrant methylation of one, or more, of the three pre-*miR-9* paralogous loci.

**MYC is involved in the regulation of miR-9 levels in MB.** Given the prominent role of aberrant MYC in MB pathogenesis (Northcott *et al*, 2012b) and its capability to directly bind to the promoter region of *miR-9* (Ma *et al*, 2010), we investigated whether MYC is involved in the regulation of miR-9 expression in MB cells. The analysis of gene expression profiles of 285 MBs revealed a statistically significant negative correlation between *miR-9* level and *MYC* expression in primary tumour samples (Figure 2A).

A similar inverse correlation was observed when the expression levels of *MYC* and *miR-9* were analysed in a representative panel of MB cell lines. The levels of *miR-9* were higher in cell lines bearing low level of *MYC* (DAOY and PFSK), whereas high-*MYC* cells (D341 and D425) showed a relatively low expression of *miR-9* (Figure 2B). To verify this finding, we examined the level of miR-9 in MB cells ectopically overexpressing MYC (DAOY-MYC) and compared it with empty-vector-transfected cells (low MYC-DAOY cells) (Stearns *et al*, 2006). MYC overexpression resulted in a 30% decrease in *miR-9* expression (Figure 2C), suggesting the involvement of MYC in the regulation of miR-9 expression in MB cells.

MYC-mediated repression of several miRNAs has been reported (Chang *et al*, 2008; Bui and Mendell, 2010), although the underlying mechanisms are not fully clarified (Frenzel *et al*, 2010). To confirm the capability of MYC to mediate a downregulation of *miR-9* in MB and to shed light on the mechanisms behind it, we investigated whether DNA methylation was required for MYC-mediated *miR-9* repression. Indeed, MYC-induced *miR-9* repression was counteracted by 5-Aza treatment, suggesting that the oncogene MYC is involved in the reduction of *miR-9* level likely by regulating the DNA methylation status of *miR-9* promoter.

***miR-9* regulates the expression of human HES1 gene in MB.** To identify putative targets for *miR-9* with potential implications in MB tumour biology, we conducted an *in silico* search using several independent databases. Among potential *miR-9* targets, based on target site conservation in humans, distinct programs identified *HES1* (hairy and enhancer of split 1) gene as a potential target for *miR-9* (Figure 3A and Supplementary Figure S2A). As HES1 has a central role in normal brain development and in MB pathogenesis (Hallahan *et al*, 2004; Dakubo *et al*, 2006; de Bont *et al*, 2008; Ingram *et al*, 2008), we decided to focus our further investigation on *miR-9*-mediated regulation of HES1.

To gain insight into the *miR-9*/HES1 interaction in MB, we compared the expression of *HES1* and *miR-9* transcripts in MB primary samples. A pilot analysis of 15 MBs revealed a slight inverse correlation between the expression of *HES1* and *miR-9* levels (Figure 3B). To further corroborate these findings, we analysed the relationship between *HES1* and *miR-9* transcripts in two independent sets of 285 and 88 primary MB tumours (Northcott *et al*, 2012b). The analysis confirmed that *miR-9* and *HES1* expression levels are inversely correlated in both data sets (Figure 3C and D; Supplementary Figure S2B and C). The analysis of MB sugroups revealed a negative correlation between *miR-9* and *HES1* across SHH, Group 3, and Group 4 MBs in both sets of MB patient samples (Figure 3E and Supplementary Figure S2D). In contrast to the other subgroups, WNT tumours demonstrated a positive correlation between *miR-9* and *HES1* expression. Although the number of WNT samples in the analysed cohort is not large enough to validate this observation, the unexpected results obtained analyzing WNT cases might reflect a distinctive microRNA signature existing within the WNT subgroup (Gokhale *et al*, 2010).

To functionally validate *miR-9* regulation of HES1 expression, we designed a luciferase reporter fused to either the wild-type *HES1* 3′UTR sequence or to a sequence that carries a mutation in the *miR-9* seed-complementary region. The expression of the wild-type luciferase reporter in 293T cells was significantly repressed by *miR-9* precursor mimics (pre-*miR-9*) compared with scrambled precursors, whereas the expression of the mutated luciferase reporter was not significantly affected, confirming the direct repression of HES1 by *miR-9* (Figure 3F). We then examined the effect of *miR-9* overexpression on HES1 protein level in MB cell lines. Ectopic restoration of low endogenous *miR-9* expression (Figure 3G) effectively triggered a 30% decrease of HES1 protein level (Figure 3H and Supplementary Figure S2E). This result was confirmed in two additional MB cell lines (Supplementary Figure S2E). Overall, these findings show that *miR-9* regulates HES1 expression and suggest *HES1* as functional target of *miR-9* in MB cells.

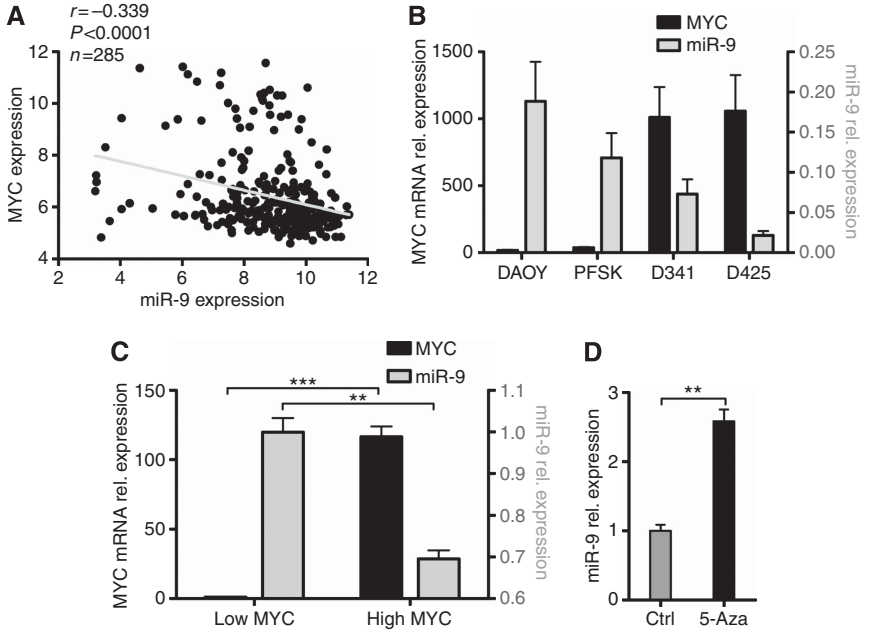


Figure 2. The oncogene MYC is involved in the regulation of miR-9 expression. (**A**) Correlation between *miR-9* and *MYC* mRNA expression in 285 MB patients' samples data sets as determined by microarray-based expression profiles (Northcott *et al*, 2012b; *r* = Pearson's correlation coefficient). (**B**) Relative mRNA expression of *MYC* (left y axis) and expression of *miR-9* (right y axis) in the indicated cell lines as determined by qRT–PCR. (**C**) Relative mRNA expression of *MYC* (left y axis) and expression of *miR-9* (right y axis) in empty-vector-transfected DAOY cells (low MYC) and in MYC-transfected DAOY cells (high MYC) as determined by qRT–PCR. (**D**) Relative expression of *miR-9* in MYC-transfected DAOY cells upon 24 h of 5-Aza treatment as determined by qRT–PCR. (*P < 0.05, **P < 0.01, ***P < 0.001 according to Student s t-test.)

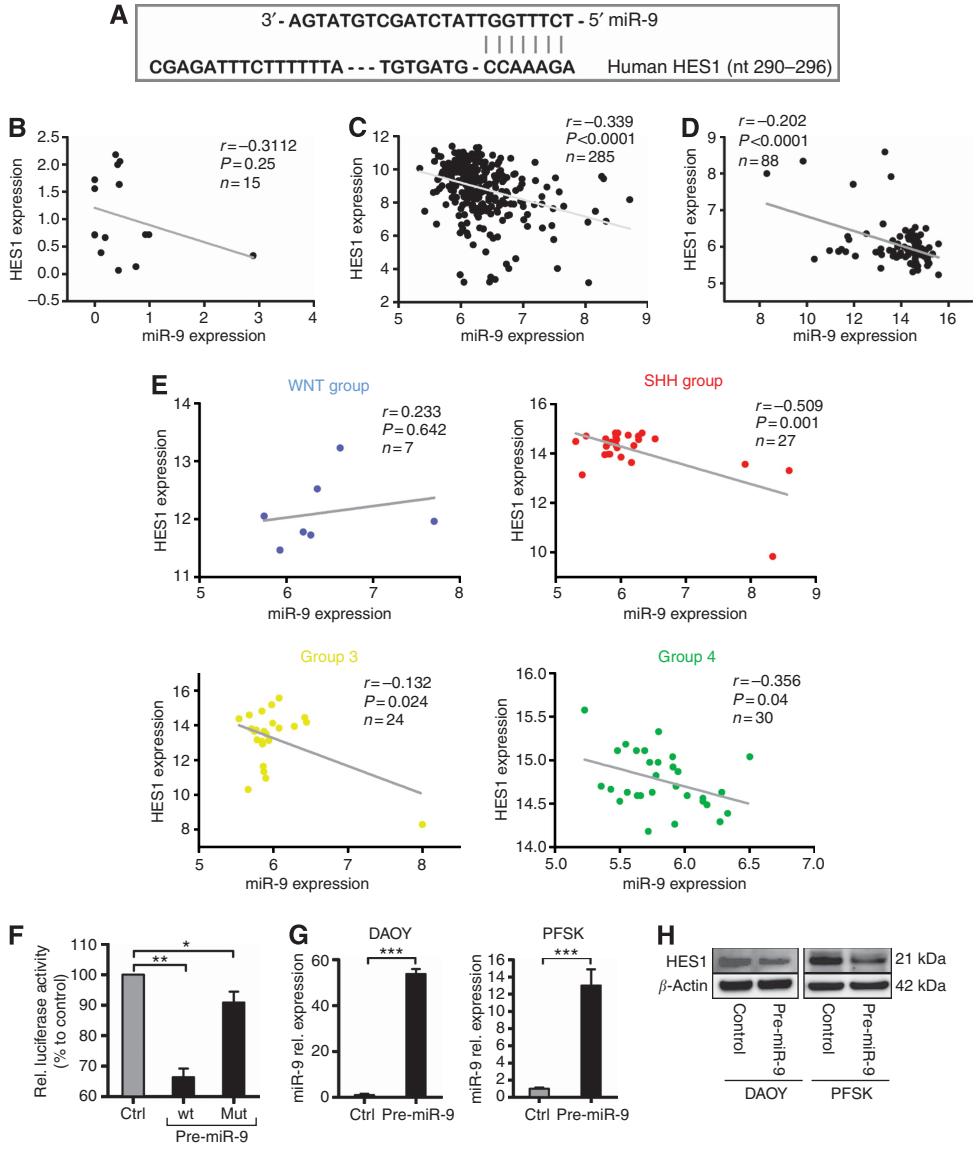


Figure 3. *miR-9* regulates HES1 expression in MB cells. (**A**) Sequence alignment of predicted *miR-9* binding site in the 3′UTR of *HES1* promoter (seed-complementary region). (**B–D**) Correlation study of *miR-9* and *HES1* expression in three independent sets of MB patients' samples as determined by qRT–PCR and by microarray-based expression profiles. ($r$ = Pearson's correlation coefficient). (**E**) Correlation study of *HES1* and *miR-9* levels according to MB subgroups (WNT, SHH, Group 3, Group 4) ($n = 88$). (**F**) Luciferase reporter activity in 293T cells transfected with pre-*miR-9* or negative control and co-transfected with the pisCheck2 vector containing the 3′UTR of *HES1* gene downstream of the firefly luciferase reporter gene. (**G**) Relative *miR-9* expression as determined by qRT–PCR 48 h following transfection with either pre-*miR-9* or control in the indicated MB cell lines. Values represent fold increase of *miR-9* mRNA relative to control. (*P <0.05, **P <0.01, ***P <0.001 according to Student's t-test.) (**H**) Pre-*miR-9* mediated downregulation of HES1 protein expression in a representative immunoblotting experiment.

***miR-9* restoration in MB cells induces cell cycle arrest and impairs clonal growth.** HES1 controls tumour cell growth through the transcriptional repression of cell cycle inhibitors, such as p21 (waf1/Cip1), which is central to cell cycle regulation and is altered in the vast majority of human cancers, including MB (Figure 4A; Kabos *et al*, 2002; Murata *et al*, 2005; Monahan *et al*, 2009). We hypothesised that by repressing HES1 *miR-9* restoration could restrict the oncogenic induction of cell cycle progression in MB cells by promoting upregulation of p21. To test this possibility, we measured cell cycle distribution, changes in p21 expression, and the capability of MB cells to grow clonally following the restoration of *miR-9*. MB cells transfected with pre-*miR-9* showed consistent changes in cell cycle distribution compared with control-transfected cells. We observed a decrease in the number of cells in S-phase and an increase of cells in G1 phase, indicative of cell cycle arrest. Analogously siRNA-mediated silencing of *HES1* decreased the number of cells in S-phase, thereby phenocopying the effects of *miR-9* overexpression (Figure 4B and C). The restoration of *miR-9* resulted in an increase of p21, both at mRNA and protein levels, when compared with control-transfected MB cells (Figure 4D). Transfection of two additional MB cell lines with pre-*miR-9* confirmed this result (Supplementary Figure S3A). Although re-establishment of *miR-9* did not affect cell viability, cell senescence (data not shown), or cell death (Supplementary Figure S3B and C), it decreased the cell capability to form colonies (Figure 4E), and it reduced the size and number of neuronal spheres (Figure 4F). Taken together, these results highlight the potential benefit of *miR-9* restoration against MB cell growth.

**Re-establishment of *miR-9* in MB cells promotes neural differentiation.** The induction of endogenous HES1 inhibits neuronal differentiation (Kageyama and Ohtsuka, 1999; Ohtsuka

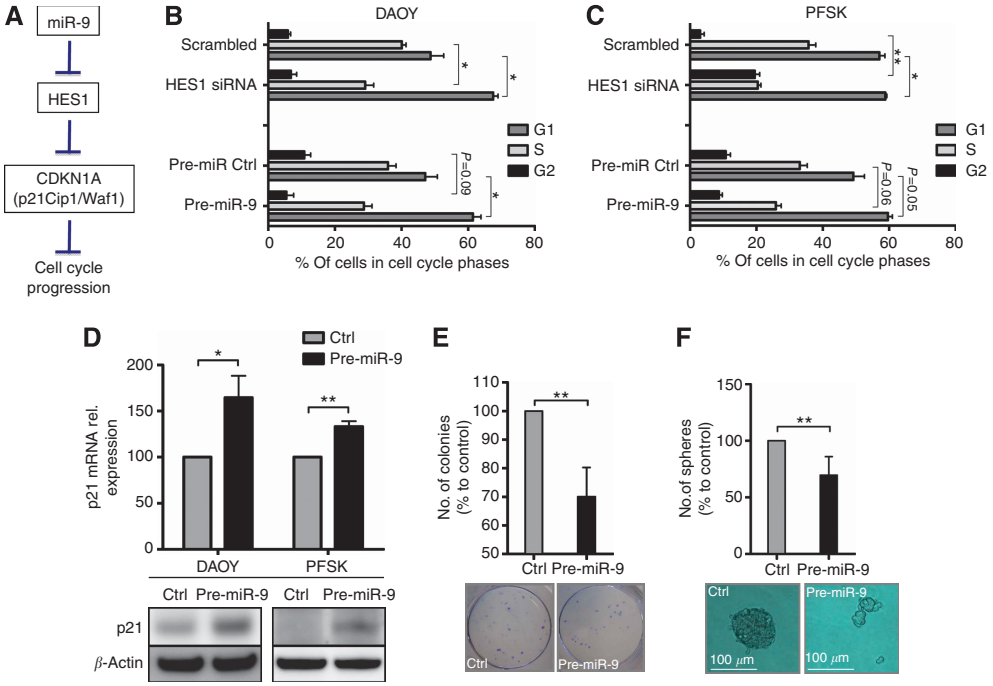


Figure 4. Restoration of *miR-9* upregulates HES1 responsive gene $P21^{Cip1}$ and impairs clonal growth of MB cells. (**A**) Cartoon depicting an overview of cell cycle-related *miR-9* downstream responsive genes and their functions. (**B**, **C**) Flow cytometric analysis of cell cycle distribution for the indicated MB cell lines 72 h after transfection with either pre-*miR-9* or control and with *HES1* siRNA or siRNA scrambled control. (**D**) Pre-miR9 mediated upregulation of p21 mRNA (upper panel) and protein (lower panels) expression in the indicated MB cell lines. (**E**) Colony formation and (**F**) sphere formation analysis of human MB DAOY cells treated with pre-*miR-9* or control for 6 days. Lower panels: representative pictures. (*P < 0.05, **P < 0.01 according to Student's t-test.)

*et al*, 1999), while HES1 knockout or mutation lead to neuronal differentiation *in vivo* (Figure 5A) (Ishibashi *et al*, 1995; Tomita *et al*, 1996). Given the important regulatory function of HES1 in neuronal differentiation (Kabos *et al*, 2002; Sang *et al*, 2008), we hypothesised that miR-9-mediated repression of HES1 could trigger the differentiation of MB cells. To test this possibility, we evaluated the effect of miR-9 restoration on MB cell differentiation. mRNA expression level of a panel of canonical neural differentiation markers were analysed by qRT–PCR: neurogenic differentiation 1 (NEUROD1) (Lee *et al*, 1995), neurofilament H (NEFH) (Lee and Cleveland, 1996), neuron-specific microtubule-associated protein (MAP2) (Dinsmore and Solomon, 1991), nestin (NES) (Wiese *et al*, 2004), β-tubulin 3 class III (TUBB3) (Katsetos *et al*, 2003), and glial fibrillary acidic protein (GFAP) (Eng *et al*, 2000). Transfection of MB cells with pre-miR-9 resulted in the upregulation of the mRNA expression of a subset of neural differentiation marker in MB cells compared with controls (Figure 5B). Among pre-miR-9-treated DAOY cells, some contacted with each other through their branching protrusions, suggesting a primary stage of differentiation (Figure 5C, upper panel), while control-treated cells retained flat morphology. Immunoflorescence analysis confirmed at the protein level that upon miR-9 re-expression both cell lines exhibited upregulation of TUBB3 and Nestin (Figure 5C and Supplementary Figure S4A) (Bhoopathi *et al*, 2011). To determine the contribution of HES1 repression to *miR-9*-mediated effects on neuronal differentiation, we examined the effects of HES1 silencing on mRNA expression of neuronal differentiation markers. As observed in MB cells treated with pre-*miR-9*, siRNA-mediated knockdown of HES1 resulted in an upregulation of a subset of neuronal differentiation genes (Supplementary Figure S4B). Similarly to the effects caused by the restoration of *miR-9*, the expression of *NeuroD1*, *Nestin*, and *GFAP* genes were upregulated by HES1 silencing. Thus, *miR-9*-mediated regulation of HES1 appears to be an essential aspect of *miR-9* function on MB cell differentiation.

To validate our results in a clinically relevant model, microarray-based expression profiling data obtained from a set of 285 MB tumours (Northcott *et al*, 2012b) were analysed searching for correlations between mRNA levels of *miR-9*, *HES1*, and previously selected neuronal differentiation markers. A trend to positively correlate was found between mRNA expression of *MAP2*, *TUBB3* and *NEUROD1* and *miR-9-2* (Figure 5D, upper panels), parallel to an inverse correlation with *HES1* mRNA expression (Figure 5D, lower panels). The analysis of the expression of *miR-9-1* and *miR-9-3* in the same MB samples also showed similar results, although less statistically significant (Supplementary Figure S4C and D).

HES1 regulatory function on cell differentiation status was previously shown to be mediated by the pro-neural differentiation gene *MASH1* (Kageyama *et al*, 1997). Therefore, we determined whether *miR-9* restoration affected the expression of MASH1. Indeed, besides the downregulation of HES1, we observed a moderate but measurable upregulation of MASH1 protein level when compared with control-transfected cells (Supplementary Figure S4E). These results suggest that *miR-9* has a critical role in MB cells by decreasing MB cell differentiation and highlight the potential use of *miR-9* restoration for reactivating the differentiation programme in cancer cells.

***miR-9* and *HES1* expression associates with clinicopathological characteristics of paediatric MB.** Finally, we investigated the association of *miR-9* and *HES1* expression with clinicopathological characteristics of paediatric MB. Three main histological subtypes of MB are included in the current WHO classification (Sarkar *et al*, 2006) among which large-cell anaplastic (LC/A) MBs represents a distinct and more aggressive variant compared with classic and desmoplastic subtypes (Leonard *et al*, 2001; von Hoff *et al*, 2010). To determine the relation of *miR-9* expression with MB histopathological subtypes, we analysed a set of MB primary samples with available information about histological features.

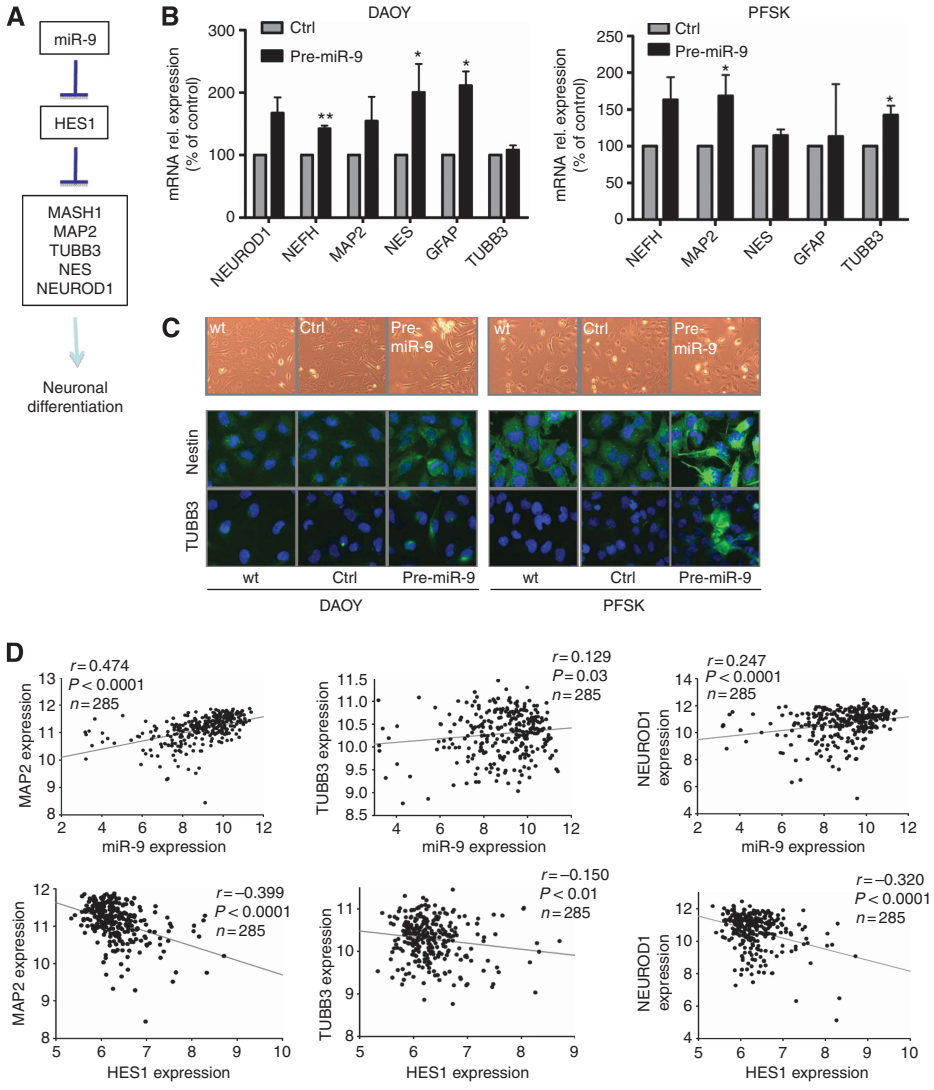


Figure 5. *miR-9* restoration mediates increase of the expression of a panel of pro-neural differentiation genes in MB cells. (**A**) Cartoon depicting an overview of neuronal differentiation-related *miR-9*/HES1 downstream responsive genes. (**B**) Relative mRNA expression of the indicated pro-neural differentiation genes as determined by qRT–PCR 72 h following transfection with either pre-*miR-9* or control. Values represent fold change relative to control (*$P<0.1$, **$P<0.01$ according to Student's *t*-test). (**C**) Morphological changes of MB cells following *miR-9* restoration and immunofluorescence analysis of *β*-tubulin class III (TUBB3) and nestin (NES) 72 h following transfection with either pre-*miR-9* or control. (**D**) Correlation study of expression of *miR-9*/*HES1* and selected pro-neural differentiation genes in 285 MB patients' samples as determined by microarray-based expression profiles ($r$ = Pearson's correlation coefficient).

Strikingly, LC/A MB samples possess lower *miR-9-2* expression compared with the other variants. In particular, a statistically significant differential expression was observed on comparing LC/A MBs with tumours of classic subtype (Figure 6A). Analysis of *miR-9-1* and *miR-9-3* expression pattern in the same MB samples showed a similar trend to inversely correlate with anaplastic MB subtypes (Supplementary Figure S5A and B), corroborating the hypothesis that MB tissues with decreased expression of *miR-9* tend to have a more severe pathological grade. Notably, LC/A MBs also showed a slightly higher *HES1* expression (Figure 6B). Furthermore, to determine the potential impact of *miR-9* on clinical outcome, *miR-9* expression level was correlated with survival. Patient survival information was available for 34 MB samples. The lower overall survival probability of patients with low *miR-9-2* expression revealed by Kaplan–Meier analysis suggests a strong trend towards prognostic significance (Figure 6C). Although it did not reach statistical significance, the analyses of *miR-9-1* and *miR-9-3* expression pattern in the same MB samples showed a similar inverse correlation between *miR-9* expression and patient's survival (Supplementary Figure S5C and D). Additionally, in line with previous reports (Cho *et al*, 2011), high *HES1* expression correlated significantly with lower overall survival in a distinct cohort of 129 MB samples (Figure 6D). We also investigated the relation between *miR-9* expression and metastatic stage, age, and gender in the same cohort of MB samples but found no significant correlation (data not shown). Together, these data indicate that low expression of *miR-9* (in particular *miR-9-2*) and the consequently increased expression of HES1 could be associated with worse MB clinical outcome. Hence, *miR-9* might be considered as a candidate marker predicting unfavourable prognosis for patients with paediatric MB that deserves further validation studies.

## DISCUSSION

The current study provides evidence that in paediatric MB *miR-9* is significantly downregulated when compared with normal fetal

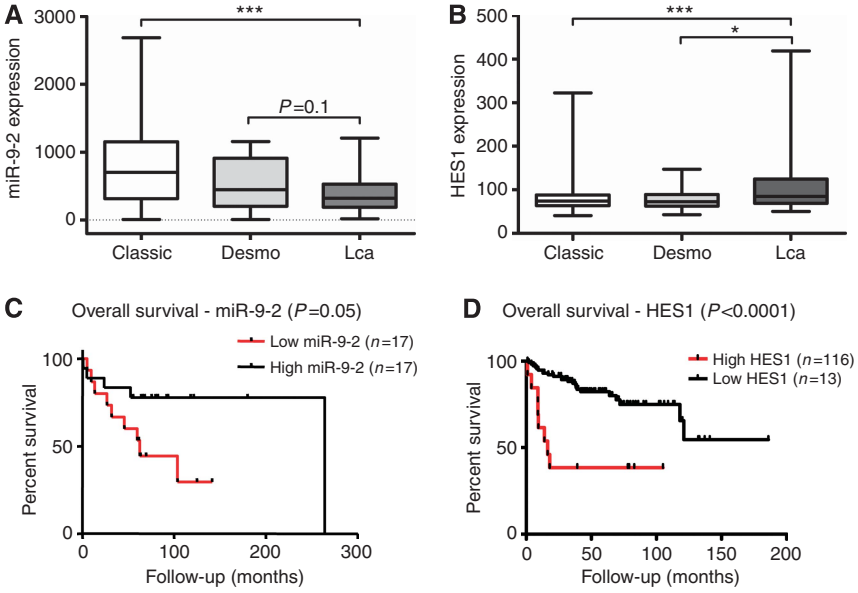


**Figure 6. Expression of *miR-9* and *HES1* are associated with clinicopatholigical characteristics of paediatric MB.** Box plots showing (**A**) *miR-9-2* and (**B**) *HES1* expression according to MB histological variants: classic ($n=200$), (desmo) desmoplastic ($n=21$) and (Lca) large cells/anaplastic ($n=30$); centre line = median. (*P<0.05, ***P<0.001 according to Student's t-test.) (**C**) Kaplan–Meier survival curves for *miR-9-2* expression in paediatric MBs. Patients were sub-divided into high ($n=17$) and low ($n=17$) *miR-9* expression groups based on the median expression value in each population. (**D**) Kaplan–Meier survival curves for *HES1* expression in paediatric MBs. Patients were sub-divided into high ($n=13$) and low ($n=116$) *HES1* expression groups based on the median expression value in each population. Optimal cutoff selection was combined with Bonferroni correction because of the low number of *HES1*-expressing tumours.

cerebellum and that *miR-9* has a tumour-suppressor role in MB tumours. We evaluated the prognostic significance of these findings, because neither the functional role nor the diagnostic implications of *miR-9* in MB have been previously defined. Our investigation revealed that the reduced expression of *miR-9* in MB cells is largely due to tumour-specific CpG promoter hypermethylation, a finding previously confirmed in other cancer types (Lehmann *et al*, 2008; Lujambio *et al*, 2008; Bandres *et al*, 2009). Epigenetic deregulation of miRNA genes highlights a potential mechanism implicated in the development of various malignancies. Considering the high frequency of methylation in *miR-9* promoter in paediatric MB we revealed in this study, the degree of promoter methylation of the *miR-9* genes could be considered as a possible useful tumour marker. Furthermore, the use of DNA-demethylating agents could have significant consequences for cancer patients, opening the possibility for new therapeutic strategies for selected patients with MB.

In MB, as in several human cancers, deregulation of the oncogene MYC is associated with tumour pathogenesis. Although in breast cancer MYC-mediated induction of miR-9 has been observed (Khew-Goodall and Goodall, 2010), our data rather suggest a potential pathological function of MYC in MB involving the repression of *miR-9* expression. This miR-9 repression likely involves epigenetic silencing, thus underlining the distinct, context-dependent regulation of miRNAs networks in different tumour backgrounds. Moreover, this observation emphasises the notion that MYC-mediated repression of tumour-suppressing miRNAs, such as *miR-9*, may be a fundamental component of the MYC tumourigenic programmes in MB, in particular in MB subgroups expressing high levels of MYC. In fact, *miR-9* downregulation was most pronounced in WNT and Group 3 tumours, which highly express the oncogene MYC. Conversely, Group 4 cases rarely express high levels of MYC (Northcott *et al*, 2011) and are characterised by an over-representation of genes involved in neuronal differentiation (Cho *et al*, 2011; Taylor *et al*, 2012). This is in accordance with our findings correlating high *miR-9* levels with induction of cell differentiation. Interestingly, Group 4 tumours are characterised by high NMYC levels, thus suggesting distinct functional significances of MYC and NMYC for miR-9 expression in MB.

Our experimental evidence shows that *HES1* is a direct target of *miR-9*-mediated translational inhibition in MB cells, corroborating a recent report about miR-9-mediated effects on the homolog of mammalian *HES1* (Hairy1) in low vertebrates (Bonev *et al*, 2012). This is highly significant because HES1, one of the main NOTCH target genes, controls cell fate decisions of the mammalian neural progenitor cells from which MBs arise (Solecki *et al*, 2001; Pomeroy *et al*, 2002). Moreover, the inverse correlation between *miR-9* and *HES1* expression across distinct independent sets of MB patients' samples is clinically relevant. A subgroup-specific analysis of *miR-9* and *HES1* expression revealed negative correlation in the non-WNT MBs. On the other hand, WNT-type MBs showed rather an increase of *miR-9* expression. This might indicate that *miR-9* has a subgroup-specific effect on translational inhibition and regulates different targets in WNT MBs, analogous to the distinctive microRNA signatures proposed within the WNT subgroup (Gokhale *et al*, 2010). Nevertheless, an analysis of a bigger cohort of WNT tumours is needed to confirm this prediction.

Our investigation showed that restoration of *miR-9* expression led to G1/S cell cycle phase arrest in MB cells and that the tumour-suppressive role of *miR-9* is mediated primarily through HES1 regulation. Thus *miR-9* restoration may reduce MB cell growth by stalling the cells in G1/S phase and preventing cell cycle progression via HES1 inhibition and p21 induction. *miR-9*-mediated inhibition of HES1 also promoted the expression of distinct neuronal differentiation markers, including early neural differentiation marker TUBB3, neural-progenitor marker Nestin, and astrocytic differentiation marker GFAP, which has been associated with less aggressive MBs and higher sensitivity to anticancer drugs (Sadatomo *et al*, 1996; Son *et al*, 2003). Indeed, our results show that *miR-9* is downregulated in poorly differentiated MB cells, whereas it is normally expressed in normal

fetal cerebellum from which MB tumours arise. Therefore, *miR-9* restoration may re-establish the neurogenic differentiation programme and reduce MB tumourigenic phenotype through the repression of HES1.

The role of *miR-9* as a prognostic factor has been recently described in different tumours, such as acute lymphocytic leukemia (Agirre et al, 2009), acute myeloid leukemia (Marcucci *et al*, 2008), and colon cancer (Schetter *et al*, 2008). Based on the analysis of primary tumour data sets, the present study suggests that *miR-9* might also be useful as a predictor of MB patient outcome. Indeed, MB patients with tumours expressing low levels of *miR-9* (and concomitantly high *HES1*) show poorer survival rates. This is in agreement with recently published reports demonstrating that high HES1 expression levels are associated with poor MB prognosis (Hallahan *et al*, 2004; Ingram *et al*, 2008). The significant association between high *HES1*/low *miR-9* expressions with established high risk indicators for MB suggests a diagnostic significance of *miR-9* expression in MB histology.

In conclusion, we identified MB-specific CpG island hypermethylation of *miR-9*, a critical regulator of MB cell differentiation and cell cycle progression. Given the dynamic and, importantly, reversible nature of DNA methylation, our results suggest that *miR-9* may serve as an important prognostic molecular marker. Furthermore, restoration of *miR-9* expression may represent a novel therapeutic strategy to contribute to improvements in the treatment of MB patients, and future studies in animal models of MB are required to evaluate miR-9-mediated regulation of MB tumour growth *in vivo*.

## ACKNOWLEDGEMENTS

We thank the Swiss Pediatric Oncology Group (SPOG) for providing medulloblastoma samples. This project was supported by the Swiss Research Foundation Child and Cancer and by Krebsliga Zürich.

## CONFLICT OF INTEREST

The authors declare no conflict of interest.

## REFERENCES

Agirre X, Vilas-Zornoza A, Jimenez-Velasco A, Martin-Subero JI, Cordeu L, Garate L, San Jose-Eneriz E, Abizanda G, Rodriguez-Otero P, Fortes P, Rifon J, Bandres E, Calasanz MJ, Martin V, Heiniger A, Torres A, Siebert R, Roman-Gomez J, Prosper F (2009) Epigenetic silencing of the tumor suppressor microRNA Hsa-miR-124a regulates CDK6 expression and confers a poor prognosis in acute lymphoblastic leukemia. *Cancer Res* **69**: 4443–4453.

Bandres E, Agirre X, Bitarte N, Ramirez N, Zarate R, Roman-Gomez J, Prosper F, Garcia-Foncillas J (2009) Epigenetic regulation of microRNA expression in colorectal cancer. *Int J Cancer* **125**: 2737–2743.

Betel D, Wilson M, Gabow A, Marks DS, Sander C (2008) The microRNA.org resource: targets and expression. *Nucleic Acids Res* **36**: D149–D153.

Bhoopathi P, Chetty C, Dontula R, Gujrati M, Dinh DH, Rao JS, Lakka SS (2011) SPARC stimulates neuronal differentiation of medulloblastoma cells via the Notch1/STAT3 pathway. *Cancer Res* **71**: 4908–4919.

Bonev B, Pisco A, Papalopulu N (2011) MicroRNA-9 reveals regional diversity of neural progenitors along the anterior-posterior axis. *Dev Cell* **20**: 19–32.

Bonev B, Stanley P, Papalopulu N (2012) MicroRNA-9 modulates Hes1 ultradian oscillations by forming a double-negative feedback loop. *Cell Rep* **2**: 10–18.

Bui TV, Mendell JT (2010) Myc: maestro of microRNAs. *Genes Cancer* **1**: 568–575.

Chang TC, Yu D, Lee YS, Wentzel EA, Arking DE, West KM, Dang CV, Thomas-Tikhonenko A, Mendell JT (2008) Widespread microRNA repression by Myc contributes to tumorigenesis. *Nat Genet* **40**: 43–50.

Cho YJ, Tsherniak A, Tamayo P, Santagata S, Ligon A, Greulich H, Berhoukim R, Amani V, Goumnerova L, Eberhart CG, Lau CC, Olson JM, Gilbertson RJ, Gajjar A, Delattre O, Kool M, Ligon K, Meyerson M, Mesirov JP, Pomeroy SL (2011) Integrative genomic analysis of medulloblastoma identifies a molecular subgroup that drives poor clinical outcome. *J Clin Oncol* **29**: 1424–1430.

Dakubo GD, Mazerolle CJ, Wallace VA (2006) Expression of Notch and Wnt pathway components and activation of Notch signaling in medulloblastomas from heterozygous patched mice. *J Neurooncol* **79**: 221–227.

de Bont JM, Packer RJ, Michiels EM, den Boer ML, Pieters R (2008) Biological background of pediatric medulloblastoma and ependymoma: a review from a translational research perspective. *Neuro-oncol* **10**: 1040–1060.

Delaloy C, Liu L, Lee JA, Su H, Shen F, Yang GY, Young WL, Ivey KN, Gao FB (2010) MicroRNA-9 coordinates proliferation and migration of human embryonic stem cell-derived neural progenitors. *Cell Stem Cell* **6**: 323–335.

Dinsmore JH, Solomon F (1991) Inhibition of MAP2 expression affects both morphological and cell division phenotypes of neuronal differentiation. *Cell* **64**: 817–826.

Dubuc AM, Mack S, Unterberger A, Northcott PA, Taylor MD (2012) The epigenetics of brain tumors. *Methods Mol Biol* **863**: 139–153.

Dweep H, Sticht C, Pandey P, Gretz N (2011) miRWalk—database: prediction of possible miRNA binding sites by 'walking' the genes of three genomes. *J Biomed Inform* **44**: 839–847.

Eng LF, Ghirnikar RS, Lee YL (2000) Glial fibrillary acidic protein: GFAP thirty-one years (1969–2000). *Neurochem Res* **25**: 1439–1451.

Esteller M (2002) CpG island hypermethylation and tumor suppressor genes: a booming present, a brighter future. *Oncogene* **21**: 5427–5440.

Fernandez LA, Northcott PA, Taylor MD, Kenney AM (2009) Normal and oncogenic roles for microRNAs in the developing brain. *Cell Cycle* **8**: 4049–4054.

Ferretti E, De Smaele E, Po A, Di Marcotullio L, Tosi E, Espinola MS, Di Rocco C, Riccardi R, Giangaspero F, Farcomeni A, Nofroni I, Laneve P, Gioia U, Caffarelli E, Bozzoni I, Screpanti I, Gulino A (2009) MicroRNA profiling in human medulloblastoma. *Int J Cancer* **124**: 568–577.

Fiaschetti G, Castelletti D, Zoller S, Schramm A, Schroeder C, Nagaishi M, Stearns D, Mittelbronn M, Eggert A, Westermann F, Ohgaki H, Shalaby T, Pruschy M, Arcaro A, Grotzer MA (2011) Bone morphogenetic protein-7 is a MYC target with prosurvival functions in childhood medulloblastoma. *Oncogene* **30**: 2823–2835.

Frenzel A, Loven J, Henriksson MA (2010) Targeting MYC-regulated miRNAs to combat cancer. *Genes Cancer* **1**: 660–667.

Gokhale A, Kunder R, Goel A, Sarin R, Moiyadi A, Shenoy A, Mamidipally C, Noronha S, Kannan S, Shirsat NV (2010) Distinctive microRNA signature of medulloblastomas associated with the WNT signaling pathway. *J Cancer Res Ther* **6**: 521–529.

Hallahan AR, Pritchard JI, Hansen S, Benson M, Stoeck J, Hatton BA, Russell TL, Ellenbogen RG, Bernstein ID, Beachy PA, Olson JM (2004) The SmoA1 mouse model reveals that notch signaling is critical for the growth and survival of sonic hedgehog-induced medulloblastomas. *Cancer Res* **64**: 7794–7800.

Hildebrandt MA, Gu J, Lin J, Ye Y, Tan W, Tamboli P, Wood CG, Wu X (2010) Hsa-miR-9 methylation status is associated with cancer development and metastatic recurrence in patients with clear cell renal cell carcinoma. *Oncogene* **29**: 5724–5728.

Hummel R, Maurer J, Haier J (2011) MicroRNAs in brain tumors: a new diagnostic and therapeutic perspective? *Mol Neurobiol* **44**: 223–234.

Ingram WJ, McCue KI, Tran TH, Hallahan AR, Wainwright BJ (2008) Sonic Hedgehog regulates Hes1 through a novel mechanism that is independent of canonical Notch pathway signalling. *Oncogene* **27**: 1489–1500.

Ishibashi M, Ang SL, Shiota K, Nakanishi S, Kageyama R, Guillemot F (1995) Targeted disruption of mammalian hairy and enhancer of split homolog-1 (HES-1) leads to up-regulation of neural helix-loop-helix factors, premature neurogenesis, and severe neural tube defects. *Genes Dev* **9**: 3136–3148.

Kabos P, Kabosova A, Neuman T (2002) Blocking HES1 expression initiates GABAergic differentiation and induces the expression of p21(CIP1/WAF1) in human neural stem cells. *J Biol Chem* **277**: 8763–8766.

Kageyama R, Ishibashi M, Takebayashi K, Tomita K (1997) bHLH transcription factors and mammalian neuronal differentiation. *Int J Biochem Cell Biol* **29**: 1389–1399.

Kageyama R, Ohtsuka T (1999) The Notch-Hes pathway in mammalian neural development. *Cell Res* **9**: 179–188.

Katsetos CD, Herman MM, Mork SJ (2003) Class III beta-tubulin in human development and cancer. *Cell Motil Cytoskeleton* **55**: 77–96.

Khew-Goodall Y, Goodall GJ (2010) Myc-modulated miR-9 makes more metastases. *Nat Cell Biol* **12**: 209–211.

Kool M, Koster J, Bunt J, Hasselt NE, Lakeman A, van Sluis P, Troost D, Meeteren NS, Caron HN, Cloos J, Mrsic A, Ylstra B, Grajkowska W, Hartmann W, Pietsch T, Ellison D, Clifford SC, Versteeg R (2008) Integrated genomics identifies five medulloblastoma subtypes with distinct genetic profiles, pathway signatures and clinicopathological features. *PLoS One* **3**: e3088.

Krek A, Grun D, Poy MN, Wolf R, Rosenberg L, Epstein EJ, MacMenamin P, da Piedade I, Gunsalus KC, Stoffel M, Rajewsky N (2005) Combinatorial microRNA target predictions. *Nat Genet* **37**: 495–500.

Laios A, O'Toole S, Flavin R, Martin C, Kelly L, Ring M, Finn SP, Barrett C, Loda M, Gleeson N, D'Arcy T, McGuinness E, Sheils O, Sheppard B, O'Leary J (2008) Potential role of miR-9 and miR-223 in recurrent ovarian cancer. *Mol Cancer* **7**: 35.

Lee JE, Hollenberg SM, Snider L, Turner DL, Lipnick N, Weintraub H (1995) Conversion of Xenopus ectoderm into neurons by NeuroD, a basic helix-loop-helix protein. *Science* **268**: 836–844.

Lee MK, Cleveland DW (1996) Neuronal intermediate filaments. *Annu Rev Neurosci* **19**: 187–217.

Lehmann U, Hasemeier B, Christgen M, Muller M, Romermann D, Langer F, Kreipe H (2008) Epigenetic inactivation of microRNA gene hsa-mir-9-1 in human breast cancer. *J Pathol* **214**: 17–24.

Leonard JR, Cai DX, Rivet DJ, Kaufman BA, Park TS, Levy BK, Perry A (2001) Large cell/anaplastic medulloblastomas and medullomyoblastomas: clinicopathological and genetic features. *J Neurosurg* **95**: 82–88.

Lewis BP, Shih IH, Jones-Rhoades MW, Bartel DP, Burge CB (2003) Prediction of mammalian microRNA targets. *Cell* **115**: 787–798.

Lujambio A, Calin GA, Villanueva A, Ropero S, Sanchez-Cespedes M, Blanco D, Montuenga LM, Rossi S, Nicoloso MS, Faller WJ, Gallagher WM, Eccles SA, Croce CM, Esteller M (2008) A microRNA DNA methylation signature for human cancer metastasis. *Proc Natl Acad Sci USA* **105**: 13556–13561.

Ma L, Young J, Prabhala H, Pan E, Mestdagh P, Muth D, Teruya-Feldstein J, Reinhardt F, Onder TT, Valastyan S, Westermann F, Speleman F, Vandesompele J, Weinberg RA (2010) miR-9, a MYC/MYCN-activated microRNA, regulates E-cadherin and cancer metastasis. *Nat Cell Biol* **12**: 247–256.

Malzkorn B, Wolter M, Liesenberg F, Grzendowski M, Stuhler K, Meyer HE, Reifenberger G (2010) Identification and functional characterization of microRNAs involved in the malignant progression of gliomas. *Brain Pathol* **20**: 539–550.

Maragkakis M, Alexiou P, Papadopoulos GL, Reczko M, Dalamagas T, Giannopoulos G, Goumas G, Koukis E, Kourtis K, Simossis VA, Sethupathy P, Vergoulis T, Koziris N, Sellis T, Tsanakas P, Hatzigeorgiou AG (2009) Accurate microRNA target prediction correlates with protein repression levels. *BMC Bioinformatics* **10**: 295.

Marcucci G, Radmacher MD, Maharry K, Mrozek K, Ruppert AS, Paschka P, Vukosavljevic T, Whitman SP, Baldus CD, Langer C, Liu CG, Carroll AJ, Powell BL, Garzon R, Croce CM, Kolitz JE, Caligiuri MA, Larson RA, Bloomfield CD (2008) MicroRNA expression in cytogenetically normal acute myeloid leukemia. *N Engl J Med* **358**: 1919–1928.

Monahan P, Rybak S, Raetzman LT (2009) The notch target gene HES1 regulates cell cycle inhibitor expression in the developing pituitary. *Endocrinology* **150**: 4386–4394.

Mulhern RK, Palmer SL, Merchant TE, Wallace D, Kocak M, Brouwers P, Krull K, Chintagumpala M, Stargatt R, Ashley DM, Tyc VL, Kun L, Boyett J, Gajjar A (2005) Neurocognitive consequences of risk-adapted therapy for childhood medulloblastoma. *J Clin Oncol* **23**: 5511–5519.

Murata K, Hattori M, Hirai N, Shinozuka Y, Hirata H, Kageyama R, Sakai T, Minato N (2005) Hes1 directly controls cell proliferation through the transcriptional repression of p27Kip1. *Mol Cell Biol* **25**: 4262–4271.

Northcott PA, Korshunov A, Pfister SM, Taylor MD (2012a) The clinical implications of medulloblastoma subgroups. *Nat Rev Neurol* **8**: 340–351.

Northcott PA, Korshunov A, Witt H, Hielscher T, Eberhart CG, Mack S, Bouffet E, Clifford SC, Hawkins CE, French P, Rutka JT, Pfister S, Taylor MD (2011) Medulloblastoma comprises four distinct molecular variants. *J Clin Oncol* **29**: 1408–1414.

Northcott PA, Shih DJ, Peacock J, Garzia L, Morrissy AS, Zichner T, Stutz AM, Korshunov A, Reimand J, Schumacher SE, Beroukhim R, Ellison DW, Marshall CR, Lionel AC, Mack S, Dubuc A, Yao Y, Ramaswamy V, Luu B, Rolider A, Cavalli FM, Wang X, Remke M, Wu X, Chiu RY, Chu A, Chuah E, Corbett RD, Hoad GR, Jackman SD, Li Y, Lo A, Mungall KL, Nip KM, Qian JQ, Raymond AG, Thiessen NT, Varhol RJ, Birol I, Moore RA, Mungall AJ, Holt R, Kawauchi D, Roussel MF, Kool M, Jones DT, Witt H, Fernandez LA, Kenney AM, Wechsler-Reya RJ, Dirks P, Aviv T, Grajkowska WA, Perek-Polnik M, Haberler CC, Delattre O, Reynaud SS, Doz FF, Pernet-Fattet SS, Cho BK, Kim SK, Wang KC, Scheurlen W, Eberhart CG, Fevre-Montange M, Jouvet A, Pollack IF, Fan X, Muraszko KM, Gillespie GY, Di Rocco C, Massimi L, Michiels EM, Kloosterhof NK, French PJ, Kros JM, Olson JM, Ellenbogen RG, Zitterbart K, Kren L, Thompson RC, Cooper MK, Lach B, McLendon RE, Bigner DD, Fontebasso A, Albrecht S, Jabado N, Lindsey JC, Bailey S, Gupta N, Weiss WA, Bognar L, Klekner A, Van Meter TE, Kumabe T, Tominaga T, Elbabaa SK, Leonard JR, Rubin JB, Liau LM, Van Meir EG, Fouladi M, Nakamura H, Cinalli G, Garami M, Hauser P, Saad AG, Iolascon A, Jung S, Carlotti CG, Vibhakar R, Ra YS, Robinson S, Zollo M, Faria CC, Chan JA, Levy ML, Sorensen PH, Meyerson M, Pomeroy SL, Cho YJ, Bader GD, Tabori U, Hawkins CE, Bouffet E, Scherer SW, Rutka JT, Malkin D, Clifford SC, Jones SJ, Korbel JO, Pfister SM, Marra MA, Taylor MD (2012b) Subgroup-specific structural variation across 1,000 medulloblastoma genomes. *Nature* **488**: 49–56.

Ohtsuka T, Ishibashi M, Gradwohl G, Nakanishi S, Guillemot F, Kageyama R (1999) Hes1 and Hes5 as notch effectors in mammalian neuronal differentiation. *EMBO J* **18**: 2196–2207.

Pang JC, Kwok WK, Chen Z, Ng HK (2009) Oncogenic role of microRNAs in brain tumors. *Acta Neuropathol* **117**: 599–611.

Piriyapongsa J, Bootchai C, Ngamphiw C, Tongsima S (2012) microPIR: an integrated database of microRNA target sites within human promoter sequences. *PLoS One* **7**: e33888.

Pomeroy SL, Tamayo P, Gaasenbeck M, Sturla LM, Angelo M, McLaughlin ME, Kim JY, Goumnerova LC, Black PM, Lau C, Allen JC, Zagzag D, Olson JM, Curran T, Wetmore C, Biegel JA, Poggio T, Mukherjee S, Rifkin R, Califano A, Stolovitzky G, Louis DN, Mesirov JP, Lander ES, Golub TR (2002) Prediction of central nervous system embryonal tumour outcome based on gene expression. *Nature* **415**: 436–442.

Sadatomo T, Yoshida J, Wakabayashi T, Mizuno M, Harada K, Kurisu K, Uozumi T, Sugita K (1996) New approach for the treatment of medulloblastoma by transfection with glial fibrillary acidic protein gene. *Surg Oncol* **5**: 69–75.

Sang L, Coller HA, Roberts JM (2008) Control of the reversibility of cellular quiescence by the transcriptional repressor HES1. *Science* **321**: 1095–1100.

Sarkar C, Deb P, Sharma MC (2006) Medulloblastomas: new directions in risk stratification. *Neurol India* **54**: 16–23.

Schetter AJ, Leung SY, Sohn JJ, Zanetti KA, Bowman ED, Yanaihara N, Yuen ST, Chan TL, Kwong DL, Au GK, Liu CG, Calin GA, Croce CM, Harris CC (2008) MicroRNA expression profiles associated with prognosis and therapeutic outcome in colon adenocarcinoma. *JAMA* **299**: 425–436.

Shibata M, Nakao H, Kiyonari H, Abe T, Aizawa S (2011) MicroRNA-9 regulates neurogenesis in mouse telencephalon by targeting multiple transcription factors. *J Neurosci* **31**: 3407–3422.

Solecki DJ, Liu XL, Tomoda T, Fang Y, Hatten ME (2001) Activated Notch2 signaling inhibits differentiation of cerebellar granule neuron precursors by maintaining proliferation. *Neuron* **31**: 557–568.

Son EI, Kim IM, Kim DW, Yim MB, Kang YN, Lee SS, Kwon KY, Suh SI, Kwon TK, Lee JJ, Kim DS, Kim SP (2003) Immunohistochemical analysis for histopathological subtypes in pediatric medulloblastomas. *Pathol Int* **53**: 67–73.

Stearns D, Chaudhry A, Abel TW, Burger PC, Dang CV, Eberhart CG (2006) c-Myc overexpression causes anaplasia in medulloblastoma. *Cancer Res* **66**: 673–681.

Taylor MD, Northcott PA, Korshunov A, Remke M, Cho YJ, Clifford SC, Eberhart CG, Parsons DW, Rutkowski S, Gajjar A, Ellison DW, Lichter P, Gilbertson RJ, Pomeroy SL, Kool M, Pfister SM (2012) Molecular subgroups of medulloblastoma: the current consensus. *Acta Neuropathol* **123**: 465–472.

Tomita K, Ishibashi M, Nakahara K, Ang SL, Nakanishi S, Guillemot F, Kageyama R (1996) Mammalian hairy and enhancer of split homolog 1 regulates differentiation of retinal neurons and is essential for eye morphogenesis. *Neuron* **16**: 723–734.

Tsai KW, Liao YL, Wu CW, Hu LY, Li SC, Chan WC, Ho MR, Lai CH, Kao HW, Fang WL, Huang KH, Lin WC (2011) Aberrant hypermethylation of miR-9 genes in gastric cancer. *Epigenetics* **6**: 1189–1197.

Turner JD, Williamson R, Almefty KK, Nakaji P, Porter R, Tse V, Kalani MY (2010) The many roles of microRNAs in brain tumor biology. *Neurosurg Focus* **28**: E3.

von Bueren AO, Shalaby T, Rajtarova J, Stearns D, Eberhart CG, Helson L, Arcaro A, Grotzer MA (2007) Anti-proliferative activity of the quassinoid NBT-272 in childhood medulloblastoma cells. *BMC Cancer* **7**: 19.

von Hoff K, Hartmann W, von Bueren AO, Gerber NU, Grotzer MA, Pietsch T, Rutkowski S (2010) Large cell/anaplastic medulloblastoma: outcome according to myc status, histopathological, and clinical risk factors. *Pediatr Blood Cancer* **54**: 369–376.

Wienholds E, Kloosterman WP, Miska E, Alvarez-Saavedra E, Berezikov E, De Bruijn E, Horvitz HR, Kauppinen S, Plasterk RH (2005) MicroRNA expression in zebrafish embryonic development. *Science* **309**: 310–311.

Wiese C, Rolletschek A, Kania G, Blyszczuk P, Tarasov KV, Tarasova Y, Wersto RP, Boheler KR, Wobus AM (2004) Nestin expression—a property of multi-lineage progenitor cells? *Cell Mol Life Sci* **61**: 2510–2522.

Yang JH, Li JH, Shao P, Zhou H, Chen YQ, Qu LH (2011) starBase: a database for exploring microRNA-mRNA interaction maps from Argonaute CLIP-Seq and Degradome-Seq data. *Nucleic Acids Res* **39**: D202–D209.

Zhu L, Chen H, Zhou D, Li D, Bai R, Zheng S, Ge W (2012) MicroRNA-9 up-regulation is involved in colorectal cancer metastasis via promoting cell motility. *Med Oncol* **29**: 1037–1043.



Supplementary Information accompanies this paper on British Journal of Cancer website (http://www.nature.com/bjc)